Adaptive trajectory tracking control of vector propulsion unmanned surface vehicle with disturbances and input saturation

Xiaojie Sun · **Guofeng Wang** · **Yunsheng Fan**

Abstract This paper presents an adaptive trajectory tracking controller with full state feedback for vector propulsion unmanned surface vehicle (USV). The controller solves the problem of strong coupling of control inputs with vector propulsion by virtual control point method. Then, a guidance trajectory is designed to avoid input saturation as much as possible. In order to be closer to the reality of USV system, the tracking controller is also designed for its actuator. When designing the trajectory tracking controller, neural network-minimum learning parameter (NN-MLP) technology and parameter adaptive correction method are used to approximate and compensate the actuator error, model uncertainty and unknown environmental disturbances. By introducing a continuously differentiable approximate saturation function, the oscillation problem caused by the discontinuous signum function in the standard sliding mode control method is avoided. Next, the Lyapunov stability analysis of designed control law shows that the controller is ultimately uniformly bounded stability. Then, the zero-dynamics stability condition of virtual control point is also proved. Finally, compared with standard method, numerical simulation results verify the effectiveness of proposed method.

Keywords Vector propulsion · Trajectory tracking · Guidance trajectory · Input saturation · Actuator control

X. Sun (✉) · G. Wang · Y. Fan
College of Marine Electrical Engineering, Dalian Maritime University, and Liaoning Province Key Laboratory of Technology and System for Intelligent Ships, Dalian 116026, China
e-mail: xjsun.phd@gmail.com

G. Wang
e-mail: gfwangsh@163.com

Y. Fan
e-mail: yunsheng@dlmu.edu.cn

1 Introduction

Trajectory tracking control of unmanned surface vehicle (USV) is one of the important research fields in ship engineering. At present, it is the most concerned research direction in the field of ship control. This growing interest stems from the need for stability, robustness and execution efficiency of USV controller systems [1,2]. The USV can be used in practical applications, including maritime surveillance [3], water rescue [4], independent exploration [5] and water quality sampling [6]. In fact, the control of vector propulsion USV is more challenging than that of fully actuated vessel, which is due to the highly coupled characteristics of vector propulsion inputs between various degrees of freedom [7,8]. Although this characteristic enhances the maneuverability of USV, the design difficulty of controller increases correspondingly. In addition, environmental disturbances, model uncertainty, and input saturation also bring great challenges to the control sys-

tem. These factors lead to the complexity of motion control of USV.

In recent years, with the rapid development of ship engineering technology, the development of USV has attracted more and more attention and obtained certain research results [9]. At first, the trajectory tracking control of fully actuated USV was studied [10]. However, most of the USVs are small ships, which are not suitable for carrying side thruster transposition. Therefore, the research direction has turned to underactuated USV [11]. Li et al. used the barrier Lyapunov method to solve the full state constraint problem in trajectory tracking control of underactuated USV [12]. In the literature [13], a model free guidance and control integrated framework is proposed to solve the continuous waypoint tracking problem under completely unknown dynamics and environmental factors. Khooban et al. extended the standard T-S fuzzy model and linear matrix inequality, which made the controller effective in reducing the tracking time and improving the robustness of the controller [14]. On the basis of the research on the trajectory tracking control of single USV, literatures [15,16] extend it to the multi-USVs formation tracking problem.

At present, scholars have studied the trajectory tracking control for USV from different aspects and achieved some results. Due to the USV sailing in complex marine environment, the external disturbances and model uncertainty will affect the trajectory tracking control performance, so it is necessary to study the trajectory tracking control with external disturbances and model uncertainty. In [17–19], to enhance the disturbance rejection and tracking accuracy of the controller, the disturbance observer, homogeneous disturbance observer, and extended state observer are used to estimate the model uncertainty and external disturbance, respectively, so as to realize the exact trajectory tracking control of the USV. Huang et al. [20] adopt reducing order extended state observer to estimate internal and external disturbances. In [21], the nonsingular sliding mode manifold is developed by the bi-limit homogeneous theory with strong robustness against lumped uncertainties. The adaptive online construction fuzzy tracking control method is used to estimate the uncertainties without exact information of dynamic model and external environment disturbances in [22]. Then, [23] solves the influence of initial error by prescribed performance function and enhance the robustness of sliding mode controller by error trans-

formation technique. In [24], the neural network is used to approximate the unknown external disturbance and uncertainty and ensures the robustness of tracking performance through error transformation function. And the radial basis function neural network and disturbance observer are used to estimate and compensate the influence of disturbances in [25]. The above method only considers the external disturbances and model uncertainty, but does not consider the influence of actuator error.

In addition, the range of any actuator is limited, so it is necessary to consider the problem of input saturation. In the integral sliding mode trajectory tracking controller designed by [18], a smooth function is employed to adaptively approximate the input saturation nonlinearity. In [26], the trajectory tracking control problem of state constraint is addressed by a tan-type Barrier Lyapunov function to avoid the constraint state reaching the boundary value. Park [27] does not use adaptive or intelligent technique, but uses auxiliary variables to deal with the problem of input saturation. These methods are to solve the nonlinear problem of input saturation. However, one of the main reasons for input saturation is the overshoot of control input caused by excessive tracking error. Therefore, avoiding excessive tracking error is also an effective way to solve the problem of input saturation. In addition, for dealing with the input saturation problem, the anti-windup compensator adjusts the controller to achieve better control performance when the control input has been saturated. The anti-windup compensator can be directly modified on the existing controller to improve the performance of whole closed-loop system under input saturation [28]. The design of anti-windup compensator has been fully discussed in [28–30]. In recent years, some scholars began to discuss the problem of fault-tolerant control in trajectory tracking of USV. In [31], the adaptive technique combined with the backstepping method is adopted to enable the actuator fault-tolerant controller to address the fault effects and the system is guaranteed to be uniformly bounded under certain actuator failure. In [32], an online fault estimator is devised to detect, isolate, and accommodate unknown faults and disturbances without using a priori knowledge, so as to achieve accurate tracking with passive fault tolerance.

Although a lot of research work has been done in terms of the trajectory tracking control of USV, their control inputs are in the form of force and torque,

without considering the influence of actuator in USV system, including actuator input saturation and actuator error. In addition, the current underactuated control inputs are independent of each other. However, in the actual ship control, especially in the form of vector propulsion, the control inputs have strong coupling relationship. Motivated by the above problems, this paper designs an adaptive trajectory tracking controller with actuator error, input saturation and input coupling.

In this paper, the virtual control point method with the zero-dynamics stability analysis is used to solve the strong coupling of control input. On this basis, the guidance trajectory is designed to enhance the ability to suppress input saturation. Considering the problem of actuator stabilization and other disturbance factors, the neural network-minimum learning parameter method is used to approximate the actuator error, external disturbance and model uncertainty. Then, the bound value of approximation error is estimated by parameter self-adaptive correction method. Finally, an adaptive sliding mode trajectory tracking controller for vector propulsion USV is designed, and the effectiveness of proposed method is verified by simulation experiment. The main contributions of the proposed trajectory tracking controller can be summarized as follows:

(1) In this paper, the coupling problem of control input is considered in the design of trajectory tracking controller, and the virtual control point method is used to solve this problem. The stability condition for control input coupling is determined by zero-dynamics stability analysis.

(2) Considering that the excessive tracking error will cause the overshoot of control input and lead to the saturation of control input, this paper designs a guidance trajectory between the desired trajectory and the vessel to avoid the excessive tracking error and ensure that the guidance trajectory can eventually converge to the desired trajectory, so as to realize the tracking of the desired trajectory and suppress the problem of input saturation.

(3) In the design of trajectory tracking controller, considering the actuator error and other disturbance factors, the neural network-minimum learning parameter method is used to approximate the actuator error, external disturbance and model uncertainty. And the bound value of approximation error is estimated by parameter self-adaptive correction
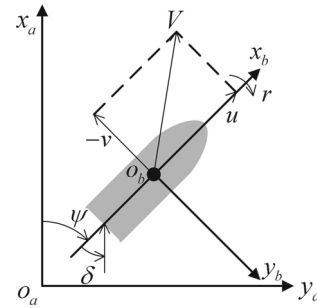

Fig. 1 The description of earth-fixed and body-fixed reference frames

correction method. In addition, for the problem of oscillation convergence of sliding mode controller caused by the discontinuity of signum function, this paper introduces a continuously differentiable approximate saturation function instead of signum function to improve the performance of controller.

The rest of this paper is organized as follows: Sect. 2 presents the mathematical model and control structure of vector propulsion USV. The adaptive trajectory tracking controller and stability analysis are provided in Sect. 3 and Sect. 4. The actuator controller is designed in Sect. 5. Simulations are carried out in Sect. 6, and conclusion is finally stated in Sect. 7.

2 Problem formulation

2.1 Mathematical model of vector propulsion USV

To study the USV motions, the Earth-fixed $o_a - x_a y_a$ and the Body-fixed $o_b - x_b y_b$ reference frames are defined in Fig. 1 [33,34].

The kinematics and dynamics equations of USV model are as follows [35,36]

$$\begin{cases} \dot{x} = u\cos\psi - v\sin\psi \\ \dot{y} = u\sin\psi + v\cos\psi \\ \dot{\psi} = r \\ \dot{u} = f_u + \Delta_u + \frac{1}{m_{11}}(T_u + b_u) \\ \dot{v} = f_v + \Delta_v + \frac{1}{m_{22}}(T_v + b_v) \\ \dot{r} = f_r + \Delta_r + \frac{1}{m_{33}}(F_r + b_r) \end{cases}, \tag{1}$$

with

$$f_u = \frac{m_{22}}{m_{11}}vr - \frac{d_{11}}{m_{11}}u$$

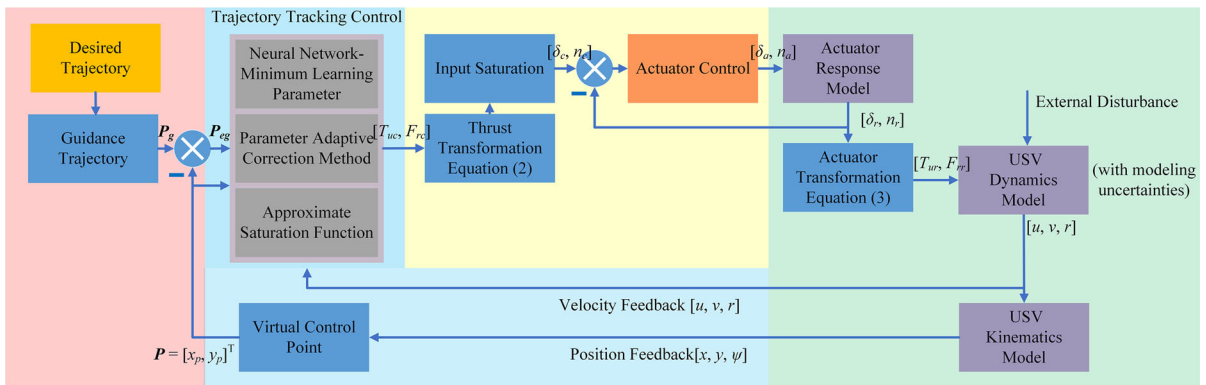$$f_v = -\frac{m_{11}}{m_{22}}ur - \frac{d_{22}}{m_{22}}v$$

Fig. 2 Control structure for vector propulsion USV

$$f_r = \frac{m_{11} - m_{22}}{m_{33}} uv - \frac{d_{33}}{m_{33}} r$$

Here, (x, y, ψ) are the vessel position and yaw angle in the earth-fixed frame, u and v are the longitudinal and transverse linear velocities in surge (body-fixed x_b) and sway (body-fixed y_b) directions, respectively, and r is the angular velocity in yaw axes in the body-fixed frame (see Fig. 1). (T_u, T_v, F_r) are the thrust (moment) component of the surge, sway, and yaw axes. m_{11}, m_{22}, m_{33} are the vessel inertia including added mass effects, and d_{11}, d_{22}, d_{33} are the hydrodynamic damping coefficients. $(\Delta_u, \Delta_v, \Delta_r)$ and (b_u, b_v, b_r) are the unmodeled dynamics and external disturbances induced by wind, waves, and ocean currents acting on surge, sway, and yaw directions.

For vector propulsion system, the thrust transformation equation showing the relationship between (T_u, T_v, F_r) and (vector propulsion angle δ, thruster speed n)is [37,38]

$$\begin{cases} T_u = T \cos(\delta) \\ T_v = -T \sin(\delta) \\ F_r = T \sin(\delta) L/2 \end{cases}, \quad (2)$$
$$T = (1 - t_p) \rho n^2 D_p^4 K_T$$

where T is the thrust of propulsion system, and L is the length of vessel hull. By solving the (2) in reverse, the actuator transformation equation [39,40] can be obtained as follows can be obtained by actuator transformation equation as

$$\begin{cases} \delta = \arctan\left(\frac{2F_r}{T_u L}\right) \\ n = \sqrt{\frac{T_u}{(1-t_p)\rho D_p^4 K_T \cos(\delta)}} \end{cases}. \quad (3)$$

As an actuator, the propulsion angle δ and thruster speed n of propulsion system need a certain response time during execution, so their response model [41,42] is

$$\begin{cases} T_q \dot{n}_r + n_r = K_q n_a \\ \ddot{\delta}_r + 2\zeta \omega_n \dot{\delta}_r + \omega_n^2 \delta_r = K_\delta \omega_n^2 \delta_a \end{cases}, \quad (4)$$

where (n_a, δ_a) and (n_r, δ_r) are the control inputs and actual outputs of actuator, respectively; T_q and K_q denote the time constant, gain of n; ω_n, ζ, and K_δ refer to the natural frequency, damping ratio, and proportionality coefficient of δ. The $n \in [0, n_m]$ and $\delta \in [-\delta_m, \delta_m]$ are the executable ranges of actuator.

2.2 Control structure

Aiming at the vector propulsion USV with the influence of input saturation, input coupling, actuator error, model uncertainty, and external disturbances in the marine environment, an adaptive trajectory tracking control with full state feedback is proposed for vector propulsion USV.

Figure 2 shows the structure of proposed controller. The controller structure diagram is divided into four blocks, including guidance trajectory block (pink), trajectory tracking control block (cyan), actuator control block (yellow), and USV model block (green). The guidance law converts the desired trajectory P_d into the guidance trajectory P_g. Control input saturation is mainly caused by large disturbances and initial state error [43,44]. To avoid the problem of control input saturation, guidance law is adopted to avoid input saturation. In the design of control structure, considering the influence of actuator error, the actuator control

is also designed, and the thrust (moment) components (T_u, T_v, F_r) and (thruster speed n, propulsion angle δ) are transformed by Eqs. (2) and (3). Considering the input coupling problem, the trajectory tracking controller is designed on the basis of virtual control point, and the disturbance effects such as actuator error, model uncertainty and unknown environment disturbances are reduced by neural network-minimum learning parameter and parameter adaptive correction method. In addition, a continuously differentiable approximate saturation function is used to avoid the oscillation caused by the signum function in controller design.

3 Trajectory tracking control

3.1 Preliminaries

In the stabilization and tracking process of the actuator, there are tracking errors between the actual control inputs $\mathbf{u_r} = [T_{ur}, F_{rr}]^T$ and command control inputs $\mathbf{u_c} = [T_{uc}, F_{rc}]^T$, so the actuator errors $\mathbf{u_e} = [T_e, F_e]^T$ for thrust and torque are $T_e = T_{ur} - T_{uc}$ and $F_e = F_{rr} - F_{rc}$.

According to (2), the dynamics equation of vessel model (1) will be modified to be

$$
\begin{cases}
\dot{u} = f_u + \frac{1}{m_{11}} T_{ur} + d_u \\
\dot{v} = f_v - \frac{2}{m_{22}L} F_{rr} + d_v \\
\dot{r} = f_r + \frac{1}{m_{33}} F_{rr} + d_r
\end{cases}
, \qquad (5)
$$

where the disturbances terms are $d_u = \Delta_u + \frac{1}{m_{11}} b_u$, $d_v = \Delta_v + \frac{1}{m_{22}} b_r$, $d_r = \Delta_r + \frac{1}{m_{33}} b_r$.

Assumption 1 The disturbances term d and actuator errors (T_e, F_e) are bounded. In other words, there exists the positive constants $\bar{d}_i$, $\bar{d}_T$ and $\bar{d}_F$, such as $|d_i| \le \bar{d}_i$, $i = u, v, r$, $|T_e| \le \bar{d}_T$ and $|F_e| \le \bar{d}_F$.

The vector propulsion mode causes the coupling problem of control inputs with (5), which makes the internal dynamics of system unstable [38,45]. Therefore, the virtual control point method is introduced to transform it into a dynamic system with internal stability. The virtual control point P is located on the longitudinal symmetrical axis of vessel with positive distance l from the geometric center as shown in Fig. 3.
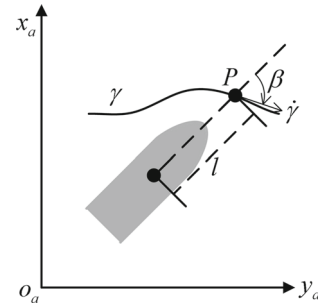

Fig. 3 The virtual control point P

The position P is given by

$$
P = \begin{bmatrix} x_p(t) \\ y_p(t) \end{bmatrix} = \begin{bmatrix} x(t) \\ y(t) \end{bmatrix} + l \begin{bmatrix} \cos \psi(t) \\ \sin \psi(t) \end{bmatrix}, l > 0. \quad (6)
$$

where $l > 0$, the reference trajectory γ of vessel tracking is represented by the desired output $P_d = [x_d(t), y_d(t)]^T$, which is generated by a virtual reference vessel with the same dynamics parameters, but without the effect of modeling uncertainties and external disturbances.

Assumption 2 The reference trajectory γ is sufficient smooth with the $x_d, \dot{x}_d, \ddot{x}_d, y_d, \dot{y}_d, \ddot{y}_d$ bounded.

Due to the excellent performance and global approximation ability of radial basis function neural network (RBFNN), it is used to approximate the unknown nonlinear disturbance term in the system.

For an arbitrary continuous function $N(X)$, the radial basis function neural network (RBFNN) can approximate it by $N(X) = W^T h(X) + \varepsilon$ with ideal weight W, input variable X, Gauss basis function h, and approximation error ε [46]. To avoid increasing the computational complexity for the on-line estimation of W, the minimal-learning parameter method is used to design the adaptive law of parameter estimation $\phi = \|W\|^2$, $\phi > 0$ instead of the weight W adjustment, with the estimated value $\hat{\phi}$ and estimation error $\tilde{\phi} = \hat{\phi} - \phi$.

The control objective is to design an adaptive tracking controller, which can ensure the uniformly ultimately bounded for the vector propulsion USV under Assumptions 1 and 2.

3.2 Guidance trajectory

Define the along and cross tracking errors between the virtual point and the desired position:

$$
\begin{bmatrix} x_e \\ y_e \end{bmatrix} = J^T(\phi_d) \begin{bmatrix} x_p - x_d \\ y_p - y_d \end{bmatrix}, \tag{7}
$$

with

$$
J(\phi_d) = \begin{bmatrix} \cos\phi_d & -\sin\phi_d \\ \sin\phi_d & \cos\phi_d \end{bmatrix},
$$

where $\phi_d = \text{atan2}(\dot{y}_d, \dot{x}_d)$.

The time derivation of x_e is

$$
\begin{aligned}
\dot{x}_e &= (\dot{x} - \dot{x}_d)\cos\phi_d - (x - x_d)\dot{\phi}_d \sin\phi_d \\
&\quad + (\dot{y} - \dot{y}_d)\sin\phi_d + (y - y_d)\dot{\phi}_d \cos\phi_d \\
&\quad - l(r - \dot{\phi}_d)\sin(\psi - \phi_d) \\
&= \dot{x}\cos\phi_d + \dot{y}\sin\phi_d - U_d + \dot{\phi}_d y_e \\
&\quad - lr\sin(\psi - \phi_d)
\end{aligned} \tag{8}
$$

where $U_d = \dot{x}_d \cos\psi_d + \dot{y}_d \sin\psi_d = \sqrt{\dot{x}_d^2 + \dot{y}_d^2}$.

According to (1), (8) can be written as

$$
\begin{aligned}
\dot{x}_e &= u\cos(\psi - \phi_d) - (v + lr)\sin(\psi - \phi_d) \\
&\quad - U_d + \dot{\phi}_d y_e \\
&= U_p \cos(\psi - \phi_d + \chi) - U_d + \dot{\phi}_d y_e
\end{aligned} \tag{9}
$$

where $U_p = \sqrt{u^2 + (v + lr)^2}$ and $\chi = \text{atan2}(v + lr, u)$.

Next, the time derivation of y_e along (1) is

$$
\begin{aligned}
\dot{y}_e &= u\sin(\psi - \phi_d) + (v + lr)\cos(\psi - \phi_d) - x_e\dot{\phi}_d \\
&= U_p \sin(\psi - \phi_d + \chi) - x_e\dot{\phi}_d
\end{aligned} \tag{10}
$$

The yaw angle and speed of designed guidance trajectory are:

$$
\begin{cases} \psi_g = \phi_d + \arctan\left(-\dfrac{y_e}{\Delta}\right) - \chi \\ U_g = \dfrac{(U_d - kx_e)\sqrt{y_e^2 + \Delta^2}}{\Delta} \end{cases} \tag{11}
$$

with $k > 0$, $\Delta > 0$. And the surge and sway velocities of designed guidance trajectory are such that

$$
\begin{cases} u_g = \sqrt{U_g^2 - v_g^2} \\ v_g = v + lr \end{cases} \tag{12}
$$

So the time derivation of designed guidance trajectory P_g can be described as

$$
\dot{P}_g = \begin{bmatrix} \dot{x}_g \\ \dot{y}_g \end{bmatrix} = J(\psi_g) \begin{bmatrix} u_g \\ v_g \end{bmatrix} \tag{13}
$$

When the following error

$$
\begin{cases} e_u = u - u_g \\ e_\psi = \psi - \psi_g \end{cases} \tag{14}
$$

converges to zero, the tracking error x_e and y_e can be guaranteed to converge to zero gradually. The proof is as follows:

The following Lyapunov function V_1 are constructed:

$$
V_1 = \frac{1}{2}x_e^2 + \frac{1}{2}y_e^2 \tag{15}
$$

Differentiating (15) along (9) and (10) gives

$$
\begin{aligned}
\dot{V}_1 &= x_e\dot{x}_e + y_e\dot{y}_e \\
&= x_e\left(U_g\cos(\psi_g - \phi_d + \chi) - U_d + \dot{\phi}_d y_e\right) \\
&\quad + y_e\left(U_g\sin(\psi_g - \phi_d + \chi) - x_e\dot{\phi}_d\right) \\
&= -kx_e^2 - U_g\frac{y_e^2}{\sqrt{\Delta^2 + y_e^2}}
\end{aligned} \tag{16}
$$

It can be obtained from (16) that $\dot{V}_1 < 0$, so the tracking error x_e and y_e are converge to zero.

3.3 Controller design

In this section, we present a constructive design technique to solve the trajectory tracking control with control input coupling problem that steers vessel systems (1) along the guidance trajectory P_g. The trajectory tracking control with virtual control point method is developed to construct feedback control input $\mathbf{u_c} = [T_{uc}, F_{rc}]^T$. We set $\chi(\psi) = [\cos\psi, \sin\psi]^T$, $o(\psi) = [-\sin\psi, \cos\psi]^T$, $R(\psi) = [\chi(\psi), o(\psi)]$. For any $x = [x_1, x_2, \cdots, x_n]^T$, $y = [y_1, y_2, \cdots, y_n]^T \in \mathbb{R}^n (n \geq 1)$, we have $\langle x, y \rangle = \sum_{i=1}^n x_i y_i$, $\|x\| = \sqrt{\langle x, x \rangle}$.

Firstly, according to Eqs. (1) and (5), the second derivative of virtual control point (6) is obtained by

$$
\begin{aligned}
\ddot{P} &= \begin{bmatrix} \ddot{x}_p \\ \ddot{y}_p \end{bmatrix} \\
&= o(\psi)ur + \chi(\psi)\left(f_u + \frac{1}{m_{11}}T_{ur} + d_u\right) \\
&\quad + o(\psi)\left(f_v - \frac{2}{m_{22}L}F_{rr} + d_v\right) - \chi(\psi)vr \\
&\quad + o(\psi)l\left(f_r + \frac{1}{m_{33}}F_{rr} + d_r\right) - \chi(\psi)lr^2
\end{aligned} \tag{17}
$$

Next, Eq. (17), written in a compact form, will be modified to be

$$\ddot{P} = F + B\mathbf{u_r} + N_0, \tag{18}$$

with

$$F = R(\psi) \begin{bmatrix} f_u - vr - lr^2 \\ f_v + ur + f_r l \end{bmatrix},$$

$$B = \left[\frac{\chi(\psi)}{m_{11}}, -o(\psi) \left(\frac{2}{m_{22}L} - \frac{l}{m_{33}} \right) \right],$$

$$\mathbf{u_r} = \mathbf{u_c} + \mathbf{u_e} = [T_{ur}, F_{rr}]^T, N_0 = R(\psi) \begin{bmatrix} d_u \\ d_v + d_r l \end{bmatrix}.$$

The control input $\mathbf{u_c}$ is designed so that the redefined output P can converge to the guidance trajectory P_g.

To this end, the target is to stabilize the $P_{eg} = P - P_g$, an adaptive sliding mode control has been proposed. To stabilize the P_{eg}, the sliding mode manifold S is defined with the form

$$S = \dot{P}_{eg} + \lambda P_{eg} + \sigma \int_0^t P_{eg}(\tau) d\tau, \tag{19}$$

where $S = [S_1, S_2]^T$, $\lambda = diag(\lambda_1, \lambda_2)$, $\lambda_i > 0$, $\sigma = diag(\sigma_1, \sigma_2)$, $\sigma_i > 0$, $i = 1, 2$.

With the design of Eq. (18), the time derivative of S can be written as

$$\dot{S} = F + B\mathbf{u_r} + N_0 - \ddot{P}_g + \lambda \dot{P}_{eg} + \sigma P_{eg}$$
$$= F + B\mathbf{u_c} + N - \ddot{P}_g + \lambda \dot{P}_{eg} + \sigma P_{eg}. \tag{20}$$

where $N = B\mathbf{u_e} + N_0$.

Then, the control law can be chosen as

$$\mathbf{u_c} = B^{-1} \left(\ddot{P}_g - \lambda \dot{P}_{eg} - \sigma P_{eg} - F - N \right). \tag{21}$$

Based on Subsection 3.1, the disturbance term N can be approached by RBFNN with the form

$$N = W^T h(X) + \varepsilon. \tag{22}$$

where the ideal weight is $W = diag(W_1, W_2)$. And according to Assumption 1, ε is bounded, so $|\varepsilon| \leq \varpi$, $\varpi > 0$. Define $\phi_i = \|W_i\|^2$, $i = 1, 2$, and update the control law

$$\mathbf{u_c} = B^{-1} \left(\ddot{P}_g - \lambda \dot{P}_{eg} - \sigma P_{eg} - F \right)$$
$$- \frac{1}{2} B^{-1} \hat{\phi} S h^T h, \tag{23}$$

with the designed adaptive law

$$\dot{\hat{\phi}}_i = \frac{\gamma_i}{2} S_i^2 h^T h - \kappa_i \gamma_i \hat{\phi}_i. \tag{24}$$

Here, $\gamma_i > 0$, $\kappa_i > 0$, $i = 1, 2$.

To ensure the convergence of sliding manifold [47], the corresponding control law with a continuously derivable approximate saturation function can be written as

$$\mathbf{u_c} = B^{-1} \left(-\frac{1}{2}\hat{\phi} S h^T h + \ddot{P}_g - \lambda \dot{P}_{eg} - \sigma P_{eg} \right)$$
$$+ B^{-1} \left(-F - \mu S - \aleph\hat{\varpi} \right) \tag{25}$$

where $\mu = diag(\mu_1, \mu_2)$, $\mu_i > 0$;

$$\aleph = diag\{sat(S_1/\vartheta_1), sat(S_2/\vartheta_2)\},$$

$$sat(S_i/\vartheta_i) = \begin{cases} sgn(S_i), & |S_i| > \frac{\vartheta_i}{\rho_i - 1} \\ \frac{\rho_i S_i}{|S_i| + \vartheta_i}, & |S| \leq \frac{\vartheta_i}{\rho_i - 1} \end{cases},$$

and $\rho_i > 1$, $\vartheta_i > 0$, $i = 1, 2$; $sgn(\cdot)$ denotes signum function.

The update law for $\hat{\varpi}$ is designed as

$$\dot{\hat{\varpi}} = \eta \left[\aleph S - \Lambda \left(\hat{\varpi} - \varpi^0 \right) \right], \tag{26}$$

where $\eta = diag(\eta_1, \eta_2)$ and $\Lambda = diag(\Lambda_1, \Lambda_2)$ are all the positive design parameter diagonal matrices. $\hat{\varpi}$ is the estimation vector of ϖ; $\varpi^0 \in \mathbf{R}^2$ is prior estimate of ϖ.

4 Stability analysis

4.1 Stability analysis for controller

Consider the following candidate Lyapunov function as

$$V_2 = \frac{1}{2} \left(S^T S + \frac{1}{\gamma_i} \sum_{i=1}^2 \tilde{\phi}_i^2 + \tilde{\varpi}^T \eta^{-1} \tilde{\varpi} \right), \tag{27}$$

where $\tilde{\phi}_i$ is the approximation error for ϕ_i such that $\tilde{\phi}_i = \hat{\phi}_i - \phi_i$, $i = 1, 2$; $\tilde{\varpi}$ is the estimation error for ϖ such as $\tilde{\varpi} = \hat{\varpi} - \varpi$.

The time derivative of V_2 can be obtained as

$$\dot{V}_2 = S^T \dot{S} + \frac{1}{\gamma_i} \sum_{i=1}^2 \tilde{\phi}_i \dot{\hat{\phi}}_i + \tilde{\varpi}^T \eta^{-1} \dot{\hat{\varpi}}. \tag{28}$$

According to (20) and (22), we can get

$$S^T \dot{S} = S^T \left(F + B\mathbf{u_r} + N_0 - \ddot{P}_g + \lambda \dot{P}_{eg} + \sigma P_{eg} \right)$$
$$= S^T \left(F + B\mathbf{u_c} + \varepsilon - \ddot{P}_g + \lambda \dot{P}_{eg} + \sigma P_{eg} \right)$$
$$+ S^T W^T h. \tag{29}$$

With $\phi_i = \|W_i\|^2$,

$$S_i^2 \phi_i h^T h + 1 = S_i^2 \|W_i\|^2 \|h\|^2 + 1$$
$$= S_i^2 \left\| W_i^T h \right\|^2 + 1 \geq 2 S_i W_i^T h. \tag{30}$$

Thus,

$$S^T \dot{S} \leq S^T \left(F + B\mathbf{u_c} + \varepsilon - \ddot{P}_g + \lambda \dot{P}_{eg} + \sigma P_{eg} \right)$$
$$+ \frac{1}{2} S^T \phi S h^T h + \frac{1}{2}. \tag{31}$$

Substituting the control law (25) into (31), which can be rewritten as

$$S^T \dot{S} \leq - S^T \mu S + S^T \varpi - S^T \aleph \hat{\varpi}$$
$$- \frac{1}{2} S^T \tilde{\phi} S h^T h + \frac{1}{2}. \tag{32}$$

Consider the adaptive law (24), we have

$$\frac{1}{\gamma_i} \tilde{\phi}_i \dot{\hat{\phi}}_i = \tilde{\phi}_i \left(\frac{1}{2} S_i^2 h^T h - \kappa_i \hat{\phi}_i \right). \tag{33}$$

Because $(\tilde{\phi}_i + \phi_i)^2 \geq 0$, then $\tilde{\phi}_i^2 + 2\tilde{\phi}_i(\hat{\phi}_i - \tilde{\phi}_i) + \phi_i^2 \geq 0$, i.e., $2\tilde{\phi}_i \hat{\phi}_i \geq \tilde{\phi}_i^2 - \phi_i^2$, so the (33) is

$$\frac{1}{\gamma_i} \tilde{\phi}_i \dot{\hat{\phi}}_i \leq \frac{1}{2} S_i^2 \tilde{\phi}_i h^T h - \frac{1}{2} \kappa_i \tilde{\phi}_i^2 + \frac{1}{2} \kappa_i \phi_i^2. \tag{34}$$

In light of update law (26), we can get

$$\tilde{\varpi}^T \eta^{-1} \dot{\hat{\varpi}} = \tilde{\varpi}^T \eta^{-1} \eta \left[\aleph S - \Lambda \left(\hat{\varpi} - \varpi^0 \right) \right]$$
$$= \tilde{\varpi}^T \aleph S - \left(\hat{\varpi} - \varpi \right)^T \Lambda \left(\hat{\varpi} - \varpi^0 \right). \tag{35}$$

According to the following inequalities,

$$- \left(\hat{\varpi} - \varpi \right)^T \Lambda \left(\hat{\varpi} - \varpi^0 \right)$$
$$= -\frac{1}{2} (\hat{\varpi} - \varpi)^T \Lambda (\hat{\varpi} - \varpi)$$
$$- \frac{1}{2} \left(\hat{\varpi} - \varpi^0 \right)^T \Lambda \left(\hat{\varpi} - \varpi^0 \right)$$
$$+ \frac{1}{2} \left(\varpi - \varpi^0 \right)^T \Lambda \left(\varpi - \varpi^0 \right). \tag{36}$$
$$\leq -\frac{1}{2} (\hat{\varpi} - \varpi)^T \Lambda (\hat{\varpi} - \varpi)$$
$$+ \frac{1}{2} \left(\varpi - \varpi^0 \right)^T \Lambda \left(\varpi - \varpi^0 \right)$$

We obtain

$$\tilde{\varpi}^T \eta^{-1} \dot{\hat{\varpi}} \leq \tilde{\varpi}^T \aleph S - \frac{1}{2} (\hat{\varpi} - \varpi)^T \Lambda (\hat{\varpi} - \varpi)$$
$$+ \frac{1}{2} \left(\varpi - \varpi^0 \right)^T \Lambda \left(\varpi - \varpi^0 \right)$$
$$\leq \tilde{\varpi}^T \aleph S - \frac{1}{2} \lambda_{\min} (\Lambda \eta) \tilde{\varpi}^T \eta^{-1} \tilde{\varpi} \tag{37}$$
$$+ \frac{1}{2} \left(\varpi - \varpi^0 \right)^T \Lambda \left(\varpi - \varpi^0 \right)$$

where $\lambda_{\min} (\bullet)$ represents the minimum eigenvalue of the matrix.

According to (32), (34) and (37), (28) can be written as

$$\dot{V}_2 \leq - S^T \mu S + S^T \varpi - S^T \aleph \varpi - \frac{1}{2} \sum_{i=1}^{2} \kappa_i \tilde{\phi}_i^2$$
$$+ \frac{1}{2} \sum_{i=1}^{2} \kappa_i \hat{\phi}_i^2 + \frac{1}{2} - \frac{1}{2} \lambda_{\min} (\Lambda \eta) \tilde{\varpi}^T \eta^{-1} \tilde{\varpi} \tag{38}$$
$$+ \frac{1}{2} \left(\varpi - \varpi^0 \right)^T \Lambda \left(\varpi - \varpi^0 \right)$$

For $S_i \aleph_i \varpi_i = S_i \varpi_i \mathrm{sat}(S_i/\vartheta_i)$, when $|S_i| > \frac{\vartheta_i}{\rho_i - 1}$, $S_i \aleph_i \varpi_i \leq |S_i| \varpi_i$; when $|S_i| \leq \frac{\vartheta_i}{\rho_i - 1}$, that is $\frac{S_i^2}{|S_i| + \vartheta_i} \leq \frac{1}{\rho_i} |S_i|$, so $S_i \aleph_i \varpi_i \leq \frac{\varpi_i \rho_i S_i^2}{|S_i| + \vartheta_i} \leq |S_i| \varpi_i$. It can be concluded that according to the continuously differentiable approximate saturation function, $S_i \aleph_i \varpi_i \leq |S_i| \varpi_i$, so

$$\dot{V}_2 \leq - S^T \mu S - \frac{1}{2} \sum_{i=1}^{2} \kappa_i \tilde{\phi}_i^2 + \frac{1}{2} \sum_{i=1}^{2} \kappa_i \hat{\phi}_i^2 + \frac{1}{2}$$
$$- \frac{1}{2} \lambda_{\min} (\Lambda \eta) \tilde{\varpi}^T \eta^{-1} \tilde{\varpi} \tag{39}$$
$$+ \frac{1}{2} \left(\varpi - \varpi^0 \right)^T \Lambda \left(\varpi - \varpi^0 \right)$$

When $q_1 = \mu$, $q_2 = \frac{1}{2} \lambda_{\min} (\Lambda \eta)$, $\nabla = \frac{1}{2} + \frac{1}{2} \sum_{i=1}^{2} \kappa_i \hat{\phi}_i^2 + \frac{1}{2} \left(\varpi - \varpi^0 \right)^T \Lambda \left(\varpi - \varpi^0 \right)$, then (39)

becomes

$$\dot{V}_2 \leq -S^T q_1 S - \frac{1}{2\gamma_i} \sum_{i=1}^{2} \gamma_i \kappa_i \tilde{\phi}_i^2 - q_2 \tilde{\varpi}^T \eta^{-1} \tilde{\varpi}$$
$$+ \nabla. \tag{40}$$

Therefore, it is obvious that the derivative of V_2 with respect to time can be rewritten as

$$\dot{V}_2 \leq -2q V_2 + \nabla, \tag{41}$$

where

$$q = \min \left\{ q_1, q_2, \frac{1}{2}\gamma_1\kappa_1, \frac{1}{2}\gamma_2\kappa_2 \right\} > 0. \tag{42}$$

Theorem 1 *Consider the kinematics equation of (1) and dynamics equation (5) with Assumptions 1 and 2, the adaptive law is designed according to (24) to approach the disturbance term N, and the parameters updating law is designed according to (26) to estimate the bound value of approximation error. Finally, the control law (25) is designed. By properly adjusting the control parameters λ, σ, μ, η, γ, κ, ϑ_1, ϑ_2, ρ_1, ρ_2 to satisfy the condition of (42), the uniform ultimately bounded stable of all variables in the closed-loop system can be guaranteed .*

Proof By solving inequality (41), the following result can be obtained.

$$0 \leq V_2(t) \leq \frac{\nabla}{2q} + \left(V_2(0) - \frac{\nabla}{2q} \right) e^{-2qt} \tag{43}$$

Therefore, $V_2(t)$ is uniformly ultimately bounded. According to (27), the variables $S, \tilde{\phi}_i, \tilde{\varpi}$ in the system are uniformly ultimately bounded, and then P_{eg} and $\dot{P}_{eg}$ are bounded. According to (13)-(16), the tracking errors x_e and y_e are bounded. The boundedness of $\hat{\phi}_i$ is obtained from the boundedness of $\tilde{\phi}_i$ and ϕ_i, the boundedness of $\hat{\varpi}$ is from the boundedness of $\tilde{\varpi}$ and ϖ, so that all variables in the closed-loop system of tracking control can be guaranteed to uniformly ultimately bounded. □

4.2 Zero-dynamics stability analysis

For the virtual control point method, the sway force caused by control input coupling will cause the insta-

bility of the control system due to the position selection of virtual control point P. In Fig. 3, the difference β between the yaw angle ψ of vessel and the reference velocity $\dot{\gamma}$ can express the state of zero dynamics. It is assumed that the virtual control point has tracked the desired trajectory, so the velocity u, v of vessel can be rewritten

$$u = U \cos(\beta), v = -lr - U \sin(\beta), \tag{44}$$

where reference speed is $U = \|\dot{\gamma}\|$. By (1) and (6), we can obtain

$$u = \langle \dot{\gamma}, \chi(\psi) \rangle, v = -lr + \langle \dot{\gamma}, o(\psi) \rangle,$$
$$\dot{u} = \langle \ddot{\gamma}, \chi(\psi) \rangle + vr, \dot{v} = -l\dot{r} + \langle \ddot{\gamma}, o(\psi) \rangle - ur. \tag{45}$$

Assume the disturbances terms $d_v = 0$, based on Eqs. (44) and (45), the second equation of (5) by linearizing it about $\beta = 0$ yields, we can give

$$l\ddot{\beta} + \left(\frac{d_{22}l + (m_{22} - m_{11})U}{m_{22}} \right) \dot{\beta} + \frac{d_{22}}{m_{22}}U\beta$$
$$= \frac{\partial}{m_{22}}\tau_r + \langle \ddot{\gamma}, o(\psi) \rangle, \tag{46}$$

and its characteristic equation is given by

$$p^2 + \left(\frac{d_{22}l + (m_{22} - m_{11})U}{m_{22}l} \right) p + \frac{d_{22}}{m_{22}l}U = 0. \tag{47}$$

The roots of (47) can be calculated by

$$r_{1,2} = \frac{-\left(\frac{d_{22}l + (m_{22}-m_{11})U}{m_{22}l}\right) \pm \sqrt{\frac{4Ud_{22}}{m_{22}l}}\sqrt{\xi - 1}}{2}, \tag{48}$$

where $\xi = \frac{(d_{22}l + (m_{22}-m_{11})U)^2}{4Ud_{22}m_{22}l}$.

When $\xi = 1$, the zero dynamics of system is critical damping with a compact form as

$$a\varsigma^2 - c\varsigma + b = 0, \tag{49}$$

where $\varsigma = \frac{U}{l}$, $a = (m_{22} - m_{11})^2$, $b = d_{22}^2$, $c = 2(m_{11} + m_{22})d_{22}$. Therefore, its roots are

$$\varsigma_1 = \frac{c - \sqrt{c^2 - 4ab}}{2a}, \varsigma_2 = \frac{c + \sqrt{c^2 - 4ab}}{2a}. \tag{50}$$

To ensure sufficient stability of the system, the position of virtual control point is $l = U/\varsigma_1 + o$ with a small positive constant o. At this time, the system enter the edge of over-damped state with $0 < U < \varsigma_1 l$ to avoid excessive under damping effect.

5 Design of actuator controller

The backstepping method enables the actuator to track the command input variables (δ_c, n_c) quickly and stably, which can be obtained by the output variables (T_{uc}, F_{rc}) of trajectory tracking controller with Eq. (3).

5.1 Propulsion angle control

Define the state variables $x_1 = \delta_r$ and $x_2 = \dot{\delta}_r$, the response model of propulsion angle in (4) is transformed into state space equation

$$\begin{cases} \dot{x}_1 = x_2 \\ \dot{x}_2 = -2\xi\omega_n x_2 - \omega_n^2 x_1 + K_\delta \omega_n^2 \delta_a \end{cases}. \quad (51)$$

Step 1: Define the propulsion angle surface

$$z_{\delta 1} = x_1 - \delta_c. \quad (52)$$

According to (51), we obtain

$$\dot{z}_{\delta 1} = x_2 - \dot{\delta}_c. \quad (53)$$

Step 2: Define the velocity error surface

$$z_{\delta 2} = x_2 - \alpha(z_{\delta 1}), \quad (54)$$

then (53) becomes

$$\dot{z}_{\delta 1} = z_{\delta 2} + \alpha(z_{\delta 1}) - \dot{\delta}_c. \quad (55)$$

To stabilize (51), the virtual control $\alpha(z_{\delta 1})$ is chosen as

$$\alpha(z_{\delta 1}) = -k_1 z_{\delta 1} + \dot{\delta}_c, \quad (56)$$

where k_1 is a positive design parameter. And

$$\dot{\alpha}(z_{\delta 1}) = -k_1(z_{\delta 2} - k_1 z_{\delta 1}) + \ddot{\delta}_c. \quad (57)$$

Consider the Lyapunov function candidate $V_{\delta 1}$ as

$$V_{\delta 1} = \frac{1}{2}z_{\delta 1}^2. \quad (58)$$

The time derivative of $V_{\delta 1}$ is

$$\begin{aligned} \dot{V}_{\delta 1} &= z_{\delta 1}(z_{\delta 2} + \alpha(z_{\delta 1}) - \dot{\delta}_c) \\ &= -k_1 z_{\delta 1}^2 + z_{\delta 1} z_{\delta 2}. \end{aligned} \quad (59)$$

From (51) and (54), we obtain

$$\begin{aligned} \dot{z}_{\delta 2} &= -2\xi\omega_n x_2 - \omega_n^2 x_1 + K_\delta \omega_n^2 \delta_a - \dot{\alpha}(z_{\delta 1}) \\ &= f(x_1, x_2) + K_\delta \omega_n^2 \delta_a - \dot{\alpha}(z_{\delta 1}) \end{aligned}, \quad (60)$$

where $f(x_1, x_2) = -2\xi\omega_n x_2 - \omega_n^2 x_1$.

Consider the Lyapunov function candidate $V_{\delta 2}$ as

$$V_{\delta 2} = V_{\delta 1} + \frac{1}{2}z_{\delta 2}^2. \quad (61)$$

The time derivative of $V_{\delta 2}$ is

$$\begin{aligned} \dot{V}_{\delta 2} &= -k_1 z_{\delta 1}^2 + z_{\delta 1} z_{\delta 2} + \dot{z}_{\delta 2} z_{\delta 2} \\ &= z_{\delta 2}\left(f(x_1, x_2) + K_\delta \omega_n^2 \delta_a - \dot{\alpha}(z_{\delta 1}) + z_{\delta 1}\right) \\ &\quad -k_1 z_{\delta 1}^2. \end{aligned} \quad (62)$$

Next, we design the following nonlinear propulsion angle tracking control law

$$\begin{aligned} \delta_a &= \frac{1}{K_\delta \omega_n^2}(-k_2 z_{\delta 2} - z_{\delta 1} - f(x_1, x_2)) \\ &\quad + \frac{1}{K_\delta \omega_n^2}\dot{\alpha}(z_{\delta 1}) \end{aligned}. \quad (63)$$

Then, (62) can be written as

$$\dot{V}_{\delta 2} = -k_1 z_{\delta 1}^2 \le 0. \quad (64)$$

Thus, the actual propulsion angle δ_r of USV can track the command propulsion angle δ_c by the control input δ_a of propulsion angle with globally uniformly asymptotically stable.

5.2 Thruster speed control

Define the state variables $x_3 = n_r$ and $x_4 = \dot{n}_r$, the response model of thruster speed in (4) is transformed into state space equation

$$\begin{cases} \dot{x}_3 = x_4 \\ \dot{x}_4 = \frac{K_q n_a - n_r}{T_q} \end{cases}. \quad (65)$$

Define the thruster speed surface

$$z_n = x_3 - n_c. \quad (66)$$

According to (65), we obtain

$$\dot{z}_n = x_4 - \dot{n}_d = \frac{K_q n_a - n_r}{T_q} - \dot{n}_c. \quad (67)$$

We design the following nonlinear thruster speed tracking control law

$$n_a = T_q \dot{n}_c / K_q + n_r - T_q k_2 z_n, \quad (68)$$

where k_2 is a positive design parameter.

Consider the Lyapunov function candidate V_n as

$$V_n = \frac{1}{2} z_n^2. \qquad (69)$$

The time derivative of V_n is

$$\dot{V}_n = \dot{z}_n z_n = -T_q k_2 z_n^2 \leq 0. \qquad (70)$$

Thus, the actual thruster speed n_r of USV can track the command thruster speed n_c by the control input n_a of thruster speed with globally uniformly asymptotically stable.

6 Simulation study

To verify the effectiveness of vector propulsion trajectory tracking controller designed in this paper, a vector propulsion USV in [42] is used for simulation. The vessel length is 7.02 m, other parameters are $m_{11} = 2652.25$, $m_{22} = 2825.29$, $m_{33} = 4201.26$, $d_{11} = 848.05$, $d_{22} = 2825.29$, $d_{33} = 22719.39$. And for response models of thruster speed and propulsion angle, their parameters are set as $T_q = 3$, $K_q = 1$, $\omega_n = 2.84$, $\zeta = 1.53$, and $K_\delta = 1.02$. Moreover, the proposed method (PM) is compared with the standard sliding mode control method (SM) [48,49] with the same parameters to highlight the advantages of proposed method. For the standard sliding mode control method, the control law (25) is replaced by

$$\begin{aligned} \mathbf{u_c} =& B^{-1} \left(\ddot{P}_g - \lambda \dot{P}_{eg} - \sigma P_{eg} - F \right) \\ &+ B^{-1} \left(-\mu S - \eta \mathrm{sgn}(S_i) \right) \end{aligned}.$$

In the simulation, the model uncertainties and external disturbances are added at 30 s. The uncertainty part of system is taken as $\Delta_i = 0.2 f_i$, $i = u, v, r$. The disturbing force and moment [50,51] produced by external wind, wave and current are taken as

$$b_u = 1000 \left[1 + 0.5 \sin(0.2t) + 0.3 \cos(0.5t) \right],$$
$$b_v = 1000[1 + 0.5 \sin(0.2t) + 0.3 \cos(0.4t)],$$
$$b_r = 1000 \left[1 + 0.2 \sin(0.1t) + 0.2 \cos(0.2t) \right].$$

The magnitudes of actuated control variables are specified in the ranges given by $n \in [0 \quad 2670] (r/min)$, $\delta \in [-5 \quad 5] (°)$.

The reference trajectory P_d is generated by the reference vessel with reference control variables, and the model parameters of reference vessel are consistent with the USV. For reference vessel, the initial state is
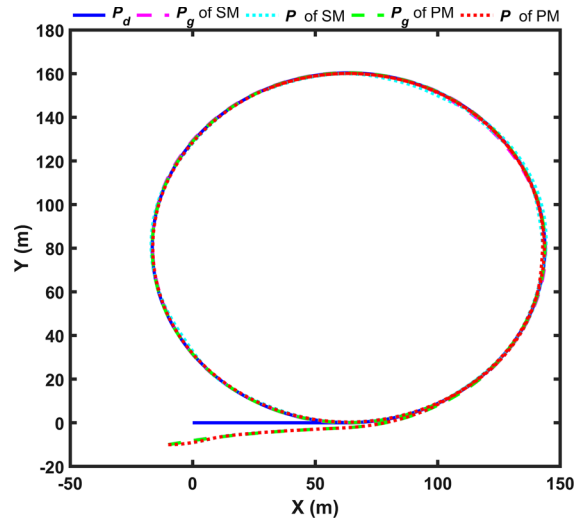

Fig. 4 Trajectory tracking result

$(x_d, y_d, \psi_d, u_d, v_d, r_d)(0) = 0$. The reference control variables are

$$n_d = 2500 \text{ r/min}, \delta_d = \begin{cases} 0°, \text{t} \leq 20 \text{ s} \\ 5°, \text{t} > 20 \text{ s} \end{cases}.$$

The initial state of USV is $(x, y, \psi, u, v, r)(0) = \{-10, -10, 0, 0, 0, 0\}$. The control point P is at the bow position with $l = U_g/\varsigma_1 + o$, $o = 0.7$. The control parameters are $\lambda = diag[0.3, 0.003]$, $\sigma = diag[0.0001, 0.0001]$, $\mu = diag[0.01, 0.1]$, $\eta = diag[0.1, 1.0]$, $\gamma = diag[10, 10]$, $\kappa = diag[0.0005, 0.0005]$, $\vartheta_1 = \vartheta_2 = 0.02$, $\rho_1 = \rho_2 = 2$, $\alpha = 0.001$ and $\Delta = 100$.

The simulation results of the standard method (SM) and proposed method (PM) are shown in Figs. 4 - 11. Fig. 4 shows the reference trajectory P_d curve, the guide trajectory P_g curve and the actual motion trajectory P curve. It can be seen from the curve in Fig. 4 that the guidance trajectory can guide the controller to smoothly and gradually track the reference trajectory under the condition of large error, thus avoiding the problem of excessive control input in the initial stage. Fig. 5 shows the curves of the velocity of surge, sway and the yaw rate vary with time. It can be seen that the proposed method can achieve accurate tracking of the desired speed, while the standard method cannot achieve accurate tracking due to the disturbance. To explain the tracking effect more clearly, according to the curves of velocity tracking error $u_e = u - u_d$, $v_e = v - v_d$, $r_e = r - r_d$ shown in Fig. 6, the velocity tracking error of the proposed method has better con-
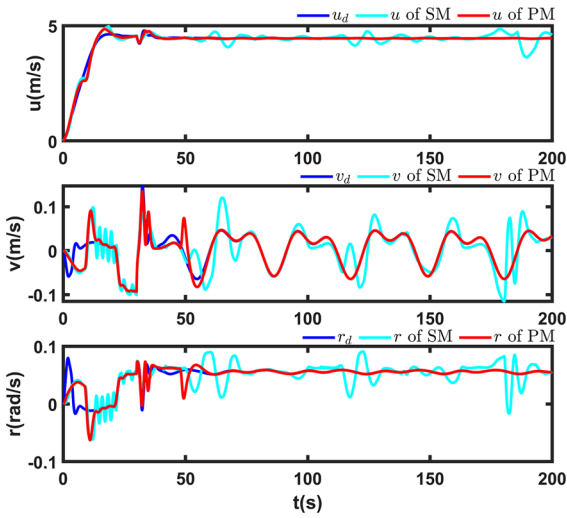
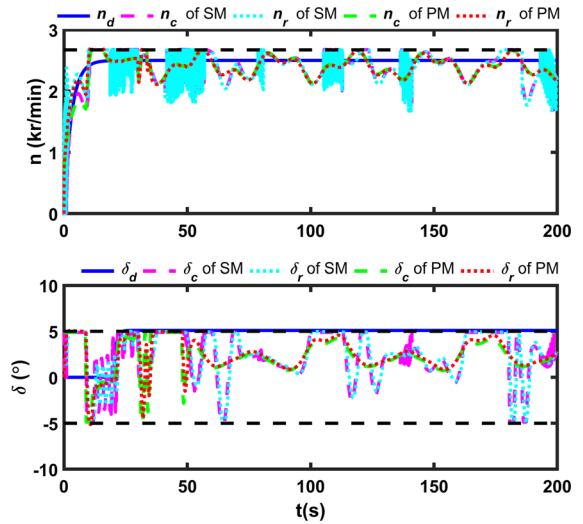**Fig. 5** Velocities of surge, sway and yaw
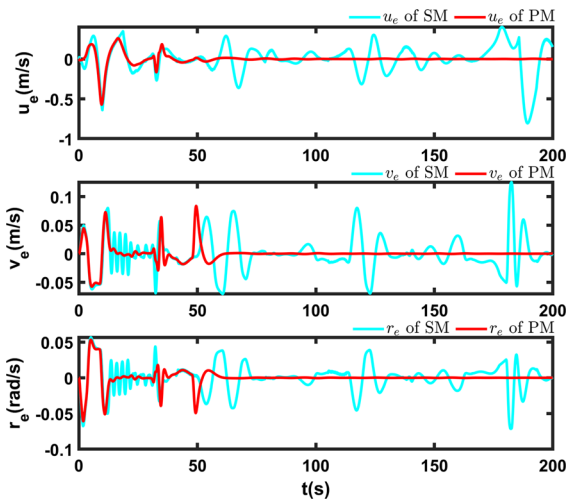

Fig. 7 Control inputs

Fig. 6 Velocity tracking errors of surge, sway and yaw
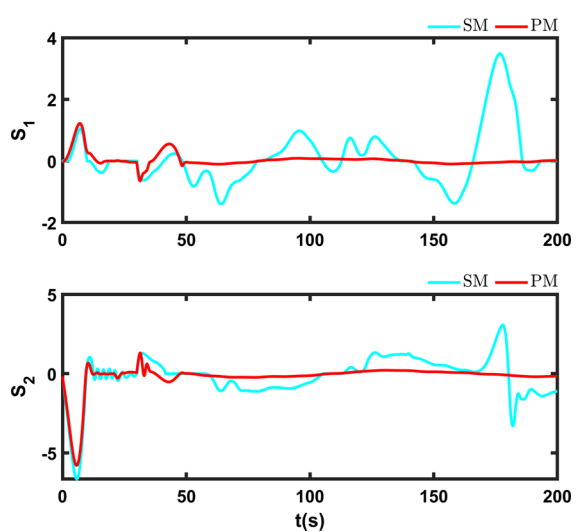

Fig. 8 Sliding mode manifold

vergence than the standard method. Fig. 7 describes the control inputs n and δ, and the black dotted line represents the input saturation value. Under the constraint of input saturation, due to the influence of disturbance factors, the control input of standard method fluctuates obviously, while the control input curve of proposed method is smoother. And it can be seen that the actual control input (n_r, δ_r) can also achieve better tracking results when tracking the command control input (n_c, δ_c) from trajectory tracking controller. Figs. 8 and 9 show sliding mode manifold (S_1, S_2) and the magnitude of tracking error $E = |P - P_d|$ in the two methods. Because the parameters of the proposed method and

standard method are completely consistent, it can be seen that the convergence curves of the two method are very similar in Figs. 8 and 9 before the model uncertainties and external disturbances are added at 30 s. However, after 30 s, the standard method is difficult to track accurately only relying on its own robustness. Although the convergence curves of the proposed method fluctuate at 30 s, they converge quickly afterward with a high precision. On the other hand, although the standard method cannot achieve accurate tracking due to model uncertainties and external disturbances, the standard method can still achieve tracking with cer-
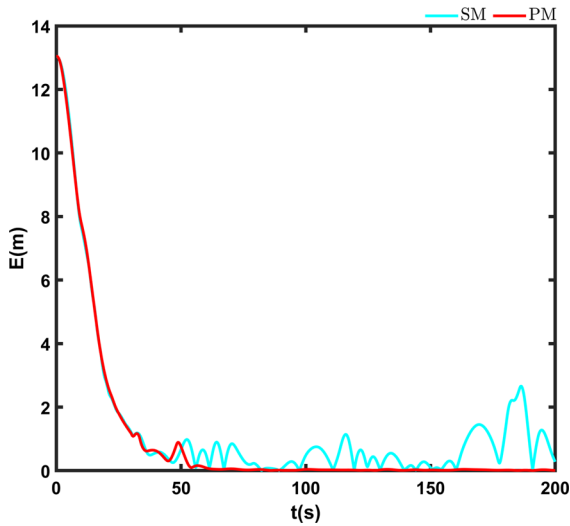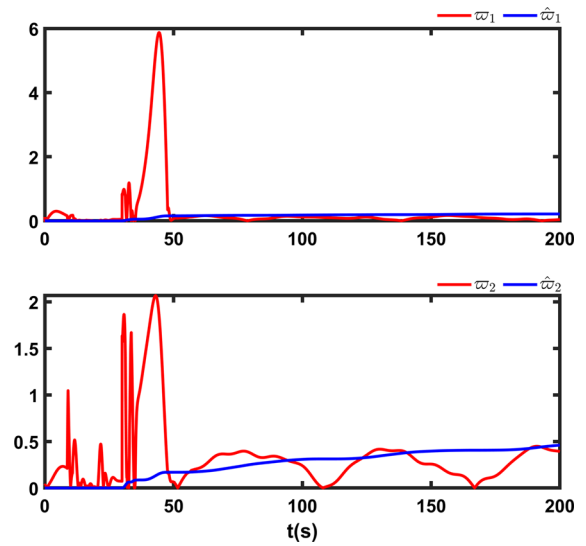
Fig. 9 The magnitude of tracking error
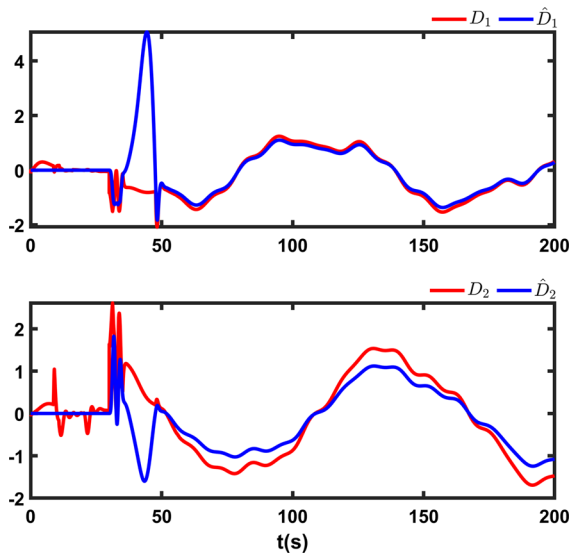

Fig. 10 The approximation curve of NN-MLP

Fig. 11 The approximation error estimation boundary

7 Conclusions

In this paper, an adaptive trajectory tracking control method is proposed for vector propulsion USV. The control strategy aims to improve the robustness of system under the influence of input saturation, input coupling, actuator error, model uncertainty and external disturbances. Comparing with the previous research, the effects associated with the actuator, including input saturation, input coupling and actuator error, are considered in the development of the trajectory tracking controller, which is more in accordance with the engineering requirements. For the input coupling problem caused by vector propulsion, the virtual control point method is used to solve, and the stability condition is obtained by zero-dynamic stability analysis. To solve the problem of input saturation, a guidance trajectory is designed between the desired trajectory and the vessel to avoid overshoot of control input due to large error. Aiming at actuator error, model uncertainty and unknown environment disturbances in vessel motion control, a neural network estimation and upper bound estimation method are proposed. In addition, in the design of controller, to reduce the oscillation of controller caused by signum function, a continuously differentiable approximate saturation function is introduced instead of the signum function. In comparison with the standard sliding mode control method, the proposed control method can not only reduce the chattering

tain errors under the guidance trajectory even if there is input saturation. Figs. 10 and 11 are the approximation of model uncertainty and environmental disturbance. It can be seen that NN-MLP can approach it well in Fig. 10, and its approximation error is estimated by ϖ in Fig. 11. Consequently, the simulation results demonstrate that the proposed controller is capable of attaining satisfactory tracking performance with the influence of input saturation, input coupling, actuator error, model uncertainty, and external disturbances.

of the error variable of E, but also make the E have a better performance and a small error, thus being more effective to be applied in the practical ship motion control for vector propulsion USV.

Note, this work naturally cannot attend to every detail of the motion controller design for vector propulsion USV, e.g., introducing anti-windup compensator to improve the performance of controller under input saturation, and fault-tolerant control for trajectory tracking with actuator failure. And considering that the selection of controller parameters will also affect the performance of the controller, to avoid adjusting too many control parameters, how to further simplify the number of controller parameters is also a very interesting problem to be discussed on the premise of ensuring that the controller has the same control performance.

Declarations

Conflict of interest The authors declare that they have no conflict of interest.

Data availability Data sharing not applicable to this article as no datasets were generated or analyzed during the current study.

References

1. Liu, Z., Zhang, Y., Yu, X., Yuan, C.: Unmanned surface vehicles: an overview of developments and challenges. Annu. Rev. Control **41**, 71–93 (2016)
2. Yoo, S.J., Park, B.S.: Guaranteed performance design for distributed bounded containment control of networked uncertain underactuated surface vessels. J. Franklin Inst. **354**(3), 1584–1602 (2017)
3. Vasilijevic, A., Nad, D., Mandic, F., Miskovic, N., Vukic, Z.: Coordinated navigation of surface and underwater marine robotic vehicles for ocean sampling and environmental monitoring. IEEE/ASME Trans. Mechatron. **22**(3), 1174–1184 (2017)
4. Jorge, V.A.M., Granada, R., Maidana, R.G., Jurak, D.A., Heck, G., Negreiros, A.P.F., dos Santos, D.H., Goncalves, L.M.G., Amory, A.M.: A survey on unmanned surface vehicles for disaster robotics: main challenges and directions. Sensors **19**(3), 702 (2019)
5. Brink, G., Garvelmann, M.: USV-UUV Swarm Vehicle Combo for Deep-Sea Exploration. Mapping. Sea Technol. **59**(8), 21–24 (2018)
6. Zhang, W., Wang, K., Wang, S.A., Laporte, G.: Clustered coverage orienteering problem of unmanned surface vehicles for water sampling. Nav. Res. Logist. **67**(5), 353–367 (2020)
7. Yao, W., Zhang, J., Liu, Y., Zhou, M., Sun, M., Zhang, G.: Improved vector control for marine podded propulsion control system based on wavelet analysis. J. Coast. Res. **73**, 54–58 (2015)
8. Gierusz, W.: Modelling the dynamics of ships with different propulsion systems for control purpose. Pol. Marit. Res. **23**(1), 31–36 (2016)
9. Zhang, G., Zhang, X.: A novel dvs guidance principle and robust adaptive path-following control for underactuated ships using low frequency gain-learning. ISA Trans. **56**, 75–85 (2015)
10. Wang, J., Liu, J.Y., Yi, H., Wu, N.L.: Adaptive non-strict trajectory tracking control scheme for a fully actuated unmanned surface vehicle. Appl. Sci. **8**(4), 598 (2018)
11. Xie, W., Ma, B., Huang, W., Zhao, Y.: Global trajectory tracking control of underactuated surface vessels with non-diagonal inertial and damping matrices. Nonlinear Dyn. **92**(4), 1481–1492 (2018)
12. Li, J.W.: Robust tracking control and stabilization of underactuated ships. Asian J. Control **20**(6), 2143–2153 (2018)
13. Wang, N., Karimi, H.R.: Successive waypoints tracking of an underactuated surface vehicle. IEEE Trans. Ind. Electron. **16**(2), 898–908 (2020)
14. Khooban, M.H., Vafamand, N., Dragicevic, T., Blaabjerg, F.: Polynomial fuzzy model-based approach for underactuated surface vessels. IET Contr. Theory Appl. **12**(7), 914–921 (2018)
15. Liang, X., Qu, X., Hou, Y., Li, Y., Zhang, R.: Distributed coordinated tracking control of multiple unmanned surface vehicles under complex marine environments. Ocean Eng. 205 (2020)
16. Dong, C., Ye, Q., Dai, S.L.: Neural-network-based adaptive output-feedback formation tracking control of USVs under collision avoidance and connectivity maintenance constraints. Neurocomputing **401**, 101–112 (2020)
17. Wang, N., Lv, S.L., Gao, Y., Er, M.J.: Disturbance/uncertainty estimation based accurate trajectory tracking control of an unmanned surface vehicle with system uncertainties and external disturbances. Indian J. Geo-marine Sci. **46**(12), 2510–2518 (2017)
18. Wang, N., Gao, Y., Lv, S., Er, M.J.: Integral sliding mode based finite-time trajectory tracking control of unmanned surface vehicles with input saturations. Indian J. Geo-marine Sci. **46**(12), 2493–2501 (2017)
19. Wang, N., Zhu, Z.B., Qin, H.D., Deng, Z.C., Sun, Y.C.: Finite-time extended state observer-based exact tracking control of an unmanned surface vehicle. Int. J. Robust Nonlinear Control **31**(5), 1704–1719 (2021)
20. Huang, H., Gong, M., Zhuang, Y., Sharma, S., Xu, D.: A new guidance law for trajectory tracking of an underactuated unmanned surface vehicle with parameter perturbations. Ocean Eng. **175**, 217–222 (2019)

21. Yao, Q.J.: Fixed-time trajectory tracking control for unmanned surface vessels in the presence of model uncertainties and external disturbances. Int. J, Control (2020)

22. Wang, S., Fu, M., Wang, Y., Tuo, Y., Ren, H.: Adaptive online constructive fuzzy tracking control for unmanned surface vessel with unknown time-varying uncertainties. IEEE Access **6**, 70444–70455 (2018)

23. Wang, S.S., Tuo, Y.L.: Robust trajectory tracking control of underactuated surface vehicles with prescribed performance. Pol. Marit. Res. **27**(4), 148–156 (2020)

24. Chen, L., Cui, R., Yang, C., Yan, W.: Adaptive neural network control of underactuated surface vessels with guaranteed transient performance: theory and experimental results. IEEE Trans. Ind. Electron. **67**(5), 4024–4035 (2020)

25. Chen, Z., Zhang, Y., Nie, Y., Tang, J., Zhu, S.: Adaptive sliding mode control design for nonlinear unmanned surface vessel using rbfnn and disturbance-observer. IEEE Access **8**, 45457–45467 (2020)

26. Li, L.L., Dong, K., Guo, G.: Trajectory tracking control of underactuated surface vessel with full state constraints. Asian J, Control (2020)

27. Park, B.S.: A simple output-feedback control for trajectory tracking of underactuated surface vessels. Ocean Eng. **143**, 133–139 (2017)

28. Akram, A., Hussain, M., us Saqib, N., Rehan, M.: Dynamic anti-windup compensation of nonlinear time-delay systems using lpv approach. Nonlinear Dyn. **90**(1), 513–533 (2017)

29. Rehan, M., Hong, K.S.: Decoupled-architecture-based nonlinear anti-windup design for a class of nonlinear systems. Nonlinear Dyn. **73**(3), 1955–1967 (2013)

30. Hussain, M., Rehan, M., Ahn, C.K., Zheng, Z.: Static antiwindup compensator design for nonlinear time-delay systems subjected to input saturation. Nonlinear Dyn. **95**(3), 1879–1901 (2019)

31. Qin, H., Li, C., Sun, Y.: Adaptive neural network-based fault-tolerant trajectory-tracking control of unmanned surface vessels with input saturation and error constraints. IET Intell. Transp. Syst. **14**(5), 356–363 (2020)

32. Wang, N., Pan, X.X., Su, S.F.: Finite-time fault-tolerant trajectory tracking control of an autonomous surface vehicle. Journal of the Franklin Institute-engineering and Applied Mathematics **357**(16), 11114–11135 (2020)

33. Yasukawa, H., Yoshimura, Y.: Introduction of mmg standard method for ship maneuvering predictions. J. Mar. Sci. Technol. **20**(1), 37–52 (2015)

34. Suzuki, R., Tsukada, Y., Ueno, M.: Estimation of full-scale ship manoeuvrability in adverse weather using free-running model test. Ocean Eng. **213**, 107562 (2020)

35. Dong, W., Guo, Y.: Global time-varying stabilization of underactuated surface vessel. IEEE Trans. Autom. Control **50**(6), 859–864 (2005)

36. Fossen, T.I.: Handbook of marine craft hydrodynamics and motion control. Wiley, London (2011)

37. Gierusz, W.: Simulation model of the lng carrier with podded propulsion part i: forces generated by pods. Ocean Eng. **108**, 105–114 (2015)

38. Consolini, L., Tosques, M.: A minimum phase output in the exact tracking problem for the nonminimum phase underactuated surface ship. IEEE Trans. Autom. Control **57**(12), 3174–3180 (2012)

39. Zhang, G.Q., Deng, Y.J., Zhang, W.D., Huang, C.F.: Novel dvs guidance and path-following control for underactuated ships in presence of multiple static and moving obstacles. Ocean Eng. **170**, 100–110 (2018)

40. Sun, X., Wang, G., Fan, Y.: Model identification and trajectory tracking control for vector propulsion unmanned surface vehicles. Electronics **9**, 22 (2020)

41. Wang, R., Zhang, J., Li, X., Liu, Y., Fu, W., Yang, Y.: Simulation study on marine main engine control based on predictive control theory. Ship Eng. **41**(S1), 165–169 (2019)

42. Sun, X., Wang, G., Fan, Y., Mu, D., Qiu, B.: Collision avoidance of podded propulsion unmanned surface vehicle with colregs compliance and its modeling and identification. IEEE Access **6**, 55473–55491 (2018)

43. Teel, Andrew: Windup in control: Its effects and their prevention (by hippe, p.; 2006). IEEE Trans. Autom. Control **53**(8), 1976–1977 (2008)

44. Hippe, P.: Windup in Control: Its Effects and Their Prevention. Springer-Verlag, New York (2006)

45. Morel, Y., Leonessa, A.: Indirect adaptive control of a class of marine vehicles. Int. J. Adapt. Control Signal Process. **24**(4), 261–274 (2010)

46. Bu, X.W., Wu, X.Y., Huang, J.Q., Ma, Z., Zhang, R.: Minimal-learning-parameter based simplified adaptive neural back-stepping control of flexible air-breathing hypersonic vehicles without virtual controllers. Neurocomputing **175**, 816–825 (2016)

47. Elmokadem, T., Zribi, M., Youcef-Toumi, K.: Trajectory tracking sliding mode control of underactuated auvs. Nonlinear Dyn. **84**(2), 1079–1091 (2016)

48. Fetzer, K.L., Nersesov, S., Ashrafiuon, H.: Full-state nonlinear trajectory tracking control of underactuated surface vessels. J. Vib. Control **26**(15–16), 1077546319895658 (2020)

49. Yu, R., Zhu, Q., Xia, G., Liu, Z.: Sliding mode tracking control of an underactuated surface vessel. IET Contr. Theory Appl. **6**(3), 461–466 (2012)

50. Pan, C.Z., Lai, X.Z., Yang, S.X., Wu, M.: A biologically inspired approach to tracking control of underactuated surface vessels subject to unknown dynamics. Expert Syst. Appl. **42**(4), 2153–2161 (2015)

51. Hu, X., Du, J.L., Sun, Y.Q.: Robust adaptive control for dynamic positioning of ships. IEEE J. Oceanic. Eng. **42**(4), 826–835 (2017)